THE ROLE OF SHEAR IN OBLIQUE IMPACTS. A. Stickle[1], P.H. Schultz[1] and D.A. Crawford[2], [1]Brown University, Department of Geological Sciences, 324 Brook Street, Providence, RI 02912-1846 (angela_stickle@brown.edu); [2]Sandia National Laboratories, Albuquerque, NM.

Introduction: Oblique impacts produce asymmetric damage patterns due to asymmetric, directed shock waves; these patterns are seen for both laboratory and planetary scale craters [1,2]. Previous laboratory and computational studies of impact-induced damaged have focused mainly on tensile failure following hypervelocity impacts. Smooth Particle Hydrodynamics (SPH) is used to model impact damage to gain a better understanding of the phenomena and processes involved [i.e. 3-5]

Though extension plays a significant role in impact-induced damage, it is also necessary to consider the role of shear failure as an important process that is observed at a variety of scales during and after impacts [6,7]. It is widely accepted that shear failure occurs during hypervelocity impacts. For example, results of SALE-2D hydrocode calculations indicate that large regions of the target fail in shear during an impact, whereas only small regions near the surface of the target fail in tension [8]. Separate studies by Senft and Stewart (2007) using the CTH hydrocode indicate regions dominated by shear failure beneath vertical impacts [9]. Experimental results also support the presence of shear-dominated failure regions [i.e. 2,10]. Here we examine this process in more detail for oblique impacts.

Strategy: The modes of failure due to a hypervelocity impact and how this failure is manifested at large scales can present a challenge for hydrocodes. The most recent version of the CTH hydrocode [11], using adaptive mesh refinement, provides a way to test conclusions about failure modes and dominant processes drawn from small scale laboratory experiments. Here we compare impacts into planar, cylindrical and spherical polymethylmethacrylate (PMMA) targets at small scale in an attempt to constrain the sequence, location and style of failure. Corresponding CTH models allow interpretation of the underlying processes involved as well as provide a benchmark for the experimental analysis.

The transparency of PMMA allows a clear view of failure patterns within the target. CTH calculations show that shear failure is a dominant process in PMMA at laboratory scales. Shock-induced tensile failure in PMMA at laboratory scales can be shown to resemble failure in basalt although shear failure significantly reduced. Nevertheless, hydrocodes reveal that shear becomes more important at larger scales. Consequently, PMMA provides an ideal material to look at the effect of shear damage during hypervelocity impacts, as well as the interaction between shear and tensile stresses.

Planar and cylindrical targets allow calibration of the relative role of various processes, providing a benchmark between the theoretical models and experimental data. Such comparisons provide a basis for the comparison between experiments and CTH models of more complicated processes within spherical bodies.

Experimental Approach: Experiments performed at the NASA Ames Vertical Gun Range (AVGR) at the NASA Ames Research Center were conducted using planar, cylindrical and spherical targets. Quarter-inch pyrex projectiles impacted into a variety of targets, including: PMMA spheres (10 cm), cylinders (10 cm diameter, 5 cm height) and blocks (15 x 15 x 6 cm) at a 30 degree impact angle. Impact velocities ranges from 5 km/s to 5.6 km/s. High-speed imaging is used to document and analyze the sequence and location of failure due to impact.

Two- and three-dimensional CTH models using identical conditions to the experiments were computed for each target type. The calculations used a mie-grüneisen equation of state for the pyrex impactor [12], PMMA target and Styrofoam base (for block experiments only). Two separate failure criteria were used within the Johnson-Cook fracture model to determine the relative roles of shear failure and extensional failure ("spallation"). Extensional failure occurs when the stresses exceed the tensile stress of the material, whereas shear failure is set to occur at specific values of plastic strain undergone by the material.

Results: The sequence and location of failure zones appearing within various targets is captured using high-speed imaging and can be compared to theoretical models. Immediately following impact in PMMA blocks, crater damage begins with an uprange "tongue" that grows downward and uprange from this region. Approximately 6 μs after impact a downrange tongue of damage begins to form as an asymmetric damage zone grows outward and downward. The downrange tongue grows and curves downward as the asymmetry increases. A zone of damage on the bottom of the block appears ~25 μs after impact, and grows outward. Damage growth ends approximately 40 μs after impact. Figure 1 shows a time-sequence showing damage growth after a 30 degree impact of ¼" pyrex sphere into the PMMA block at ~ 5 km/s.

For cylindrical targets, damage around and beneath the impact grows asymmetrically. "Tongues" similar to those seen in planar targets appear downrange as the damage zone grows behind the shock front. Deep, downrange failure appears and grows inward as shock

waves reflect from the curved surfaces and begin to interact, ~ 40 µs after impact. For spherical targets, the downrange tongue of damage occurs immediately after impact. A shallow damage haze appears antipodal to the impact point ~30 µs after impact (Fig. 2)

Discussion: Theoretical models of laboratory-scale experiments show that shear dominates the failure process, the question of scaling always remains. CTH calculations of large-scale impacts (incorporating self-gravity) reveal that large regions beneath the crater fail due to shear stresses [13]. These calculations also show that the shallow downrange failure region seen in spherical targets is due to shear stresses, rather than shallow near-surface spallation (Fig. 3). Comparative CTH calculations for planar and cylindrical PMMA targets show that the region beneath the crater also is dominated by shear failure, with extension occuring only at crater edges and on far sides of the target.

Conclusions: Preliminary conclusions can be drawn from the above discussions. 1: Laboratory experiments into PMMA targets show that shear is a dominant failure process during and directly following a hypervelocity impact; 2: Small scale laboratory experiments into spheres and complimentary planetary-scale CTH models show that shear dominates failure following impact; 3: Downrange failure observed during oblique impacts into spheres is due to shallow shear failure behind the initial shock. This is seen in laboratory experiments with PMMA at small scale as well as CTH models at large scale for natural materials; 4: Antipodal damage is initiated at the antipode to the point of impact rather than the crater center [14].

References: [1] Schultz, P.H. and Anderson, R.R. (1996) *Geol. Soc. Of Amer. Spec. Paper*, **302**, Boulder, CO; [2] Dahl, J.M. and P.H. Schultz (2001), *Int. J. Impact Eng.*, **26,** 145-155; [3] Benz, W. and Asphaug, E. (1995), *Computer Phys. Comm.*, **87**, 253-265; [4] Benz, W. and Asphaug, E. (1994), *Icarus*, **107,** 98-116; [5] Nakamura, A. and Fujiwara, A. (1991), *Icarus*, **92**, 132-146; [6] Kenkmann, T. (2002), *Geology*, **30,** 231-234; [7] Spray, J.G. and Thompson, L.M. (1995), *Nature*, **373,** 130-132; [8] Ivanov, B.A. et al. (1997), *Int. J. Impact Eng.*, **20**, 411-430; [9] Senft, L.E. and Stewart, S.T. (2007), *J. Geo. Res.*, **112,** E11002; [10] Gupta, Y.M. (1980), *J. Appl. Phys.*, **51**, 5352-5361; [11] McGlaun, J.M., S.L. Thompson and M.G. Elrick (1990), *Int. J. Impact Eng.*, **10**, 351-360; [12] Marsh (1980), *LASL Shock Hugoniot Data*, p. 394; [13] Schultz, P.H. and Crawford, D.A. (2008) *LPS XXXIX*, Abstract #2451; [14] Schultz, P.H. (2007) *LPS XXXVIII*, Abstract #1839

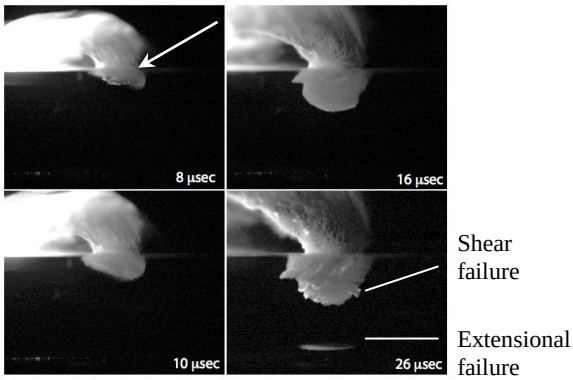

Figure 1. Time sequence of damage growth following the 30 degree impact of a ¼" pyrex sphere into a PMMA block at ~5 km/s. Downrange damage appears first, and the zone grows downward and uprange. ~25 µs after impact, extensional damage is seen on the bottom of the target. White arrow shows impact trajectory. Shear failure dominates beneath crater, and small region of extensional failure is seen at the bottom of the target.

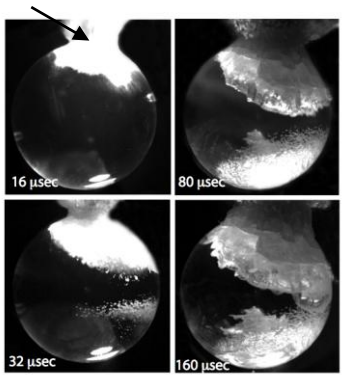

Figure 2. Time sequence of damage growth following the 30 degree impact of a ¼" pyrex sphere into a PMMA sphere at ~5 km/s. Shallow damage haze appears antipodal to the impact point. The black arrow shows impact trajectory. Bright spot on bottom of the sphere is a reflection from due to lighting conditions.

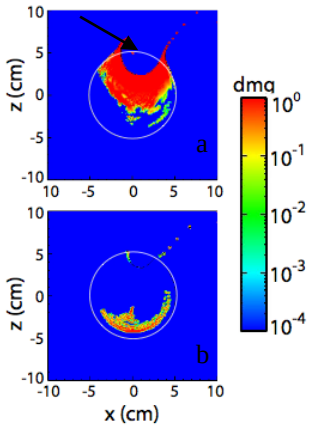

Figure 3. Oblique impact of ¼" pyrex sphere onto 4" PMMA sphere, showing the damaged regions. The black arrow shows impact trajectory. The white circle shows the original sphere shape for reference.
a) Shear failure is dominant beneath crater.
b) Extensional failure dominates on far side of target. Spallation is not occurring directly beneath the crater.